Electronic Supplementary Material (ESI) for Chemical Communications.

High entropy alloy for water oxidation: A new class of electrocatalysts to lookout

Ravi Nandan,[1] Mahendrakar. Y. Rekha,[2] Hemam Rachna Devi,[1] Chandan Srivastava[2] and Karuna Kar Nanda[1,]*A

[1]Dr. Ravi Nandan, Hemam Rachna Devi, Prof. Karuna Kar Nanda

Materials Research Centre

Indian Institute of Science

Bangalore, PIN-560012, India.

Fax: +91-80-2360 7316; **Ph:** +91-80-2293 2996

[2] M. Y. Rekha, Prof. Chandan Srivastava

Materials Engineering,

Indian Institute of Science

Bangalore, PIN-560012, India.

Correspondence:- nanda@iisc.ac.in (Prof. K. K. Nanda)

Electrochemical characterization

Water oxidation/oxygen evolution reaction (OER) studies were performed using a traditional three-electrode cell system (CHI752, USA), wherein the working electrode was the modified commercial glassy carbon electrode (GCE, active geometrical area ~ 0.07 cm^2 which was the rotating disk electrode (RDE), CHI instruments) covered by active materials (S95:5/S80:20/S50:50) with Nafion® as a binder (5%, Sigma Aldrich) solution. Platinum (Pt) ring was used as counter electrode and KCl saturated Ag/AgCl as a reference electrode. A stock ink solution of each sample was prepared by taking 7 mg of the materials dispersed by sonication (~ 1 h) in 1ml mixture of milli-Q water and ethanol (50:50%) solution. 100 µL of this ink solution was then transferred to other plastic vial with 20 µL of commercially available Nafion® binder solution followed by a sonication of 15 minutes. This catalyst ink solutions was drop-casted on the active area of glassy carbon electrode with the help of micropipette (to achieve the desired catalyst loading) followed by a drying under IR lamp. For comparative study all the potentials used in the present study are converted with respect to reversible hydrogen electrode (RHE) using the equation $E_{RHE} = E_{o\ Ag/AgCl} + (0.059 \times pH) + E_{Ag/AgCl}$, where $E_{o\ Ag/AgCl}$ is 0.197 V *vs.* SHE.[1]

The water oxidation/OER study was performed in an alkaline (1 M NaOH) aqueous solution purged for 15 minutes with nitrogen gas prior to experiment. Potential scan speed used was 10 mV/s and working electrode rotation speed of 1200 rpm in the potential range of 0 to 0.8 V vs Ag/AgCl. For The Tafel slope calculations, a current window of 5-15 mA/cm^2 was used across the electrocatalysts for uniformity. To estimate the double layer capacitance (C_{dl}), cyclic voltammetry study was performed in non-faradic region at different potential scan speed. As the all recorded OER current were

normalized with active geometrical surface area of working electrodes the loading of RuO_2 catalyst used for comparative studies was kept the same as that for S95:5, S80:20 and S50:50.

For the poisoning test, first we started the OER study in 1 M NaOH aqueous solution with a fres working electrode. After the 25 five cycles we paused the system and without disturbing the arrangment gentely introduced NaCN in the aqueous solution of NaOH. The amount of NACN was taken in such a way that the over all solution becomes 10 mM. After resuming the experiment, we observed a noticable reduction in OER current density after 25 cycles (Figure 5c Main text). For cleaning the electrode after next 25 cycles of OER in NaCN, the poisoned solution was replaced by fresh milli-Q water without removing or disturbing the working electrode and the working electrode was rotated at 1200 rpm for 10 minutes. This process was repeated for 3 times, each time fresh milli-Q water was used for cleaning. After this the elctrode was exposed to fresh 1 M NaOH aqueous solution for further OER study.

The OER performance on S95:5, S80:20 and S50:50 has been also studied in neutral, 0.1 M and 30 wt.% KOH aqueous solution (Figure S5-8). A 3.5 wt.% NaCl aqueous solution was used as a neutral medium in the present study (Figure S6).

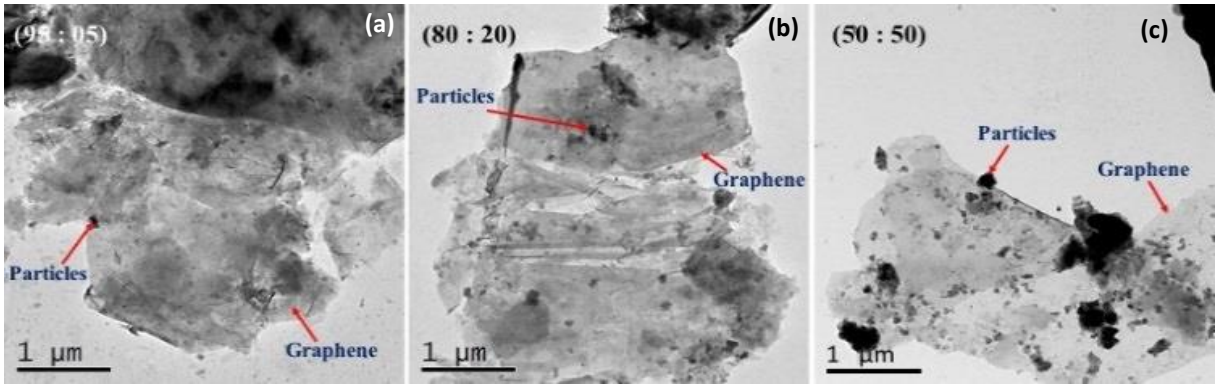

Figure S1. The representative low magnification bright-field TEM images of (a) S95:05, (b) S80:20 and (c) S50:50.

Table S1. Compositional analysis of FeCoNiCuCr HEA nanoparticles in different composites.

Composites	Cu (at. %)	Co (at. %)	Cr (at. %)	Fe (at. %)	Ni (at. %)
S95:05	18.8	18.2	9.1	30.2	23.6
S80:20	21.1	14.9	10.7	32.9	20.1
S50:50	30.8	28.4	12.8	18.7	9.1

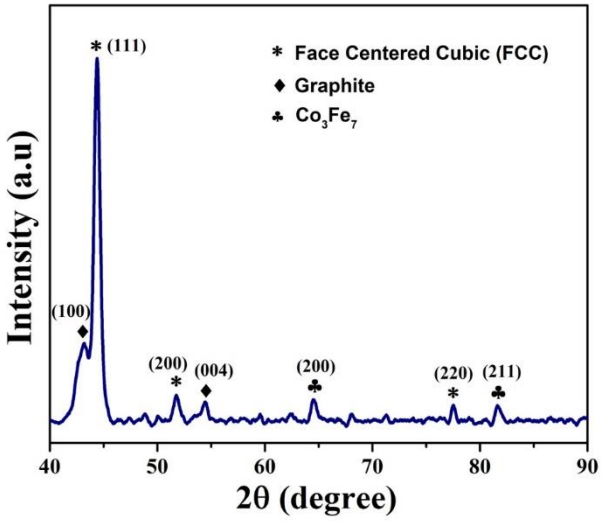

Figure S2. XRD pattern for S50:50. It clearly indicates the dominance of face centred cubic phase of FeCoNiCuCr nanoparticles.

The average crystallite size obtained from the Scherrer formula[2] and the full width half maximum (FWHM) of the fcc (111) peak was found to be 14 nm. This average crystallite size was in accordance with the average particle size as indicated in the size distribution histogram obtained for the S50:50 graphene-nanoparticle composite (Figure1f) from TEM study.

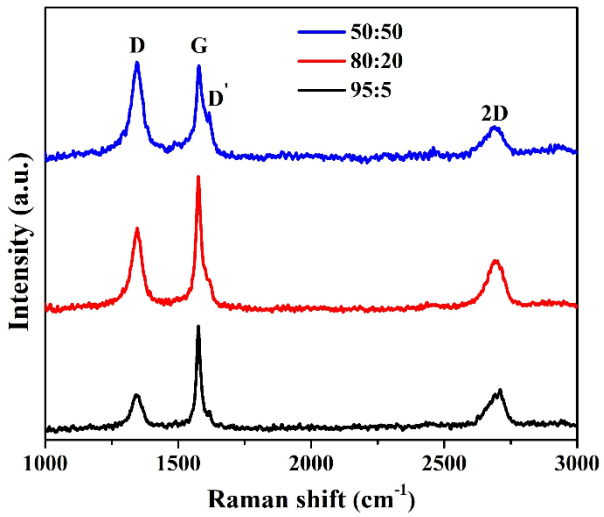

Figure S3. Raman spectra of graphene-HEA nanocomposites.

The Raman spectra were acquired using HORIBA JOBIN-YVON, LabRaman HR system consisting of a solid-state laser operating at 532 nm. Figure S3 shows the Raman spectra of all the three graphene-HEA nanocomposites. The D and D′ bands represent defects in sp^3 carbon atoms. The G and 2D bands represent in-plane vibrations of sp^2 hybridized carbon atoms and two phonon lattice vibrations respectively.[3] The defect density (I_D/I_G ratio) of 95:5, 80:20 and 50:50 graphene-HEA nanoparticles were found to be 0.71, 0.81 and 1.01 respectively. The increase in defect density is due to the increased amount of metal nanoparticle content within the graphene sheets.

Table S2. Summary of Raman studies on graphene-HEA nanocomposites. (X represents the respective peak position (cm^{-1}) and Y is the concomitant intensity of peak.)

Samples	I_D	I_G	I_{2D}	I_D/I_G
95:5	X = 1342.3 Y = 136.73	X = 1576.1 Y = 192.24	X = 2710.9 Y = 140.81	0.7112
80:20	X = 1345.5 Y = 175.69	X = 1576.1 Y = 217.47	X = 2689.0 Y = 149.43	0.8078
50:50	X = 1345.1 Y = 202.85	X = 1577.7 Y = 199.91	X = 2687.4 Y = 150.309	1.0147

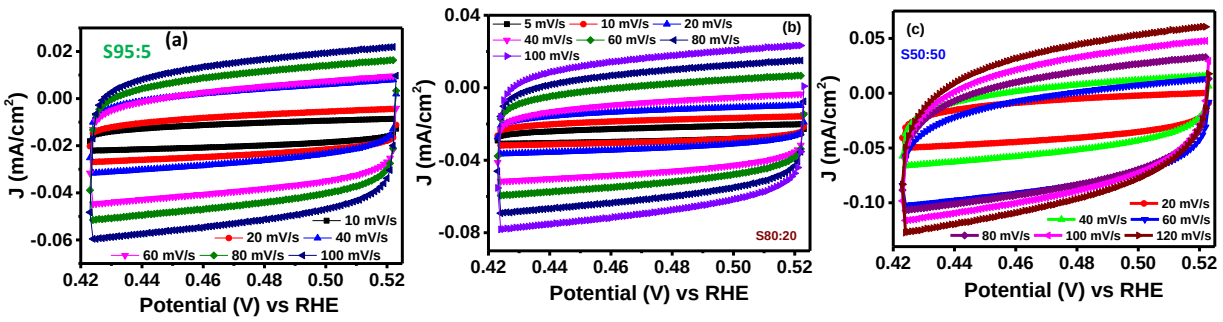

Figure S4. CV curves recorded in non-Faradic region on (a) S95:5, (b) S80:20 and (c) S50:50 in 1 M NaOH aqueous solution for double layer capacitance evaluation.

Table S3. Summary of water oxidation performance of various electrocatalysts in alkaline medium.

Composites	E_{onset} (V)	$E_{J=10}$ (V)	Tafel slope (mV/dec)	$J_{specific\ activity}$ (mA/cm^2) @ 1.75 V	$J_{Mass\ activity}$ (mA/mg) @ 1.75 V
S95:05	1.55	1.6	94	66	190
S80:20	1.53	1.58	91	87	247
S50:50	1.515	1.56	80	149	380
RuO_2	1.51	1.575	114	68	193

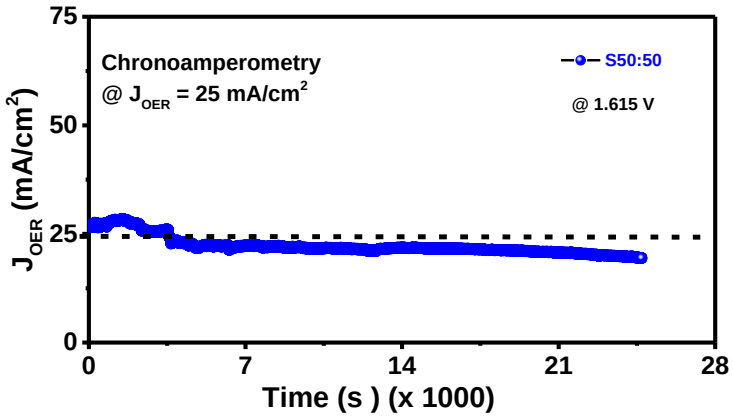

Figure S5. Chronoamperometric study on S50:50 at a current density of ~ 25 mA/cm^2 in nitrogen saturated alkaline (1 M NaOH) aqueous solution. The working electrode rotational speed was 1200 rpm during the measurement.

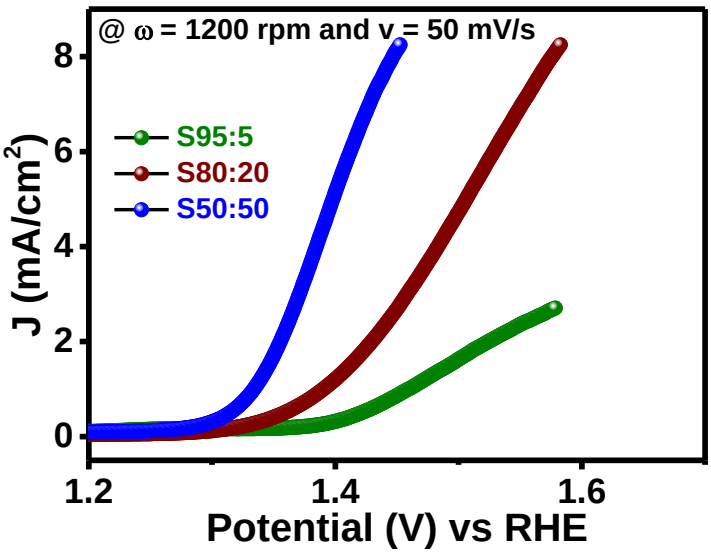

Figure S6. OER polarization curves for S95:5, S80:20 and S50:50 in neutral aqueous solution.

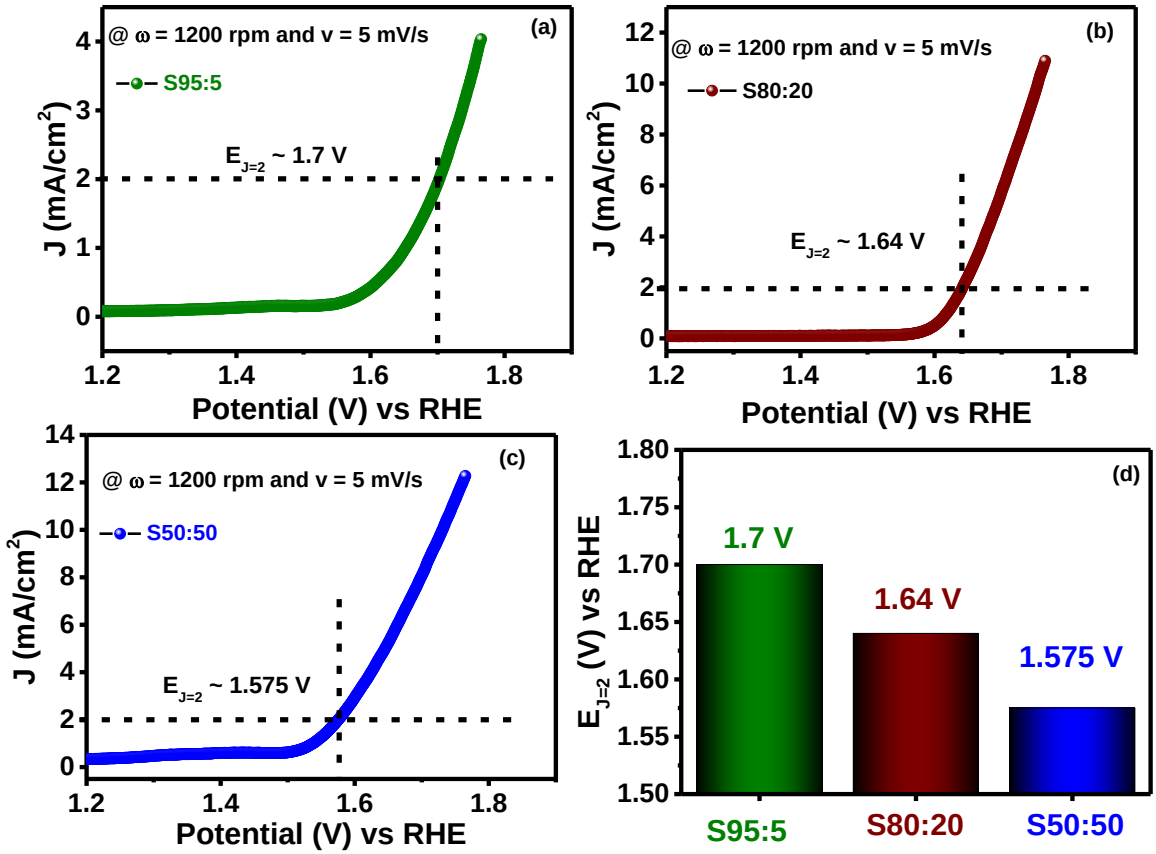

Figure S7. OER polarization curves for (a) S95:5, (b) S80:20 and (c) S50:50, in 0.1 M KOH aqueous solution. (d) The potential required for different electrocatalysts to achieve a current density of 2 mA/cm^2 as deduced from Figure S7a-c. The experimental findings suggest that S50:50 have comparatively better electrochemical water oxidation capability under identical experimental conditions.

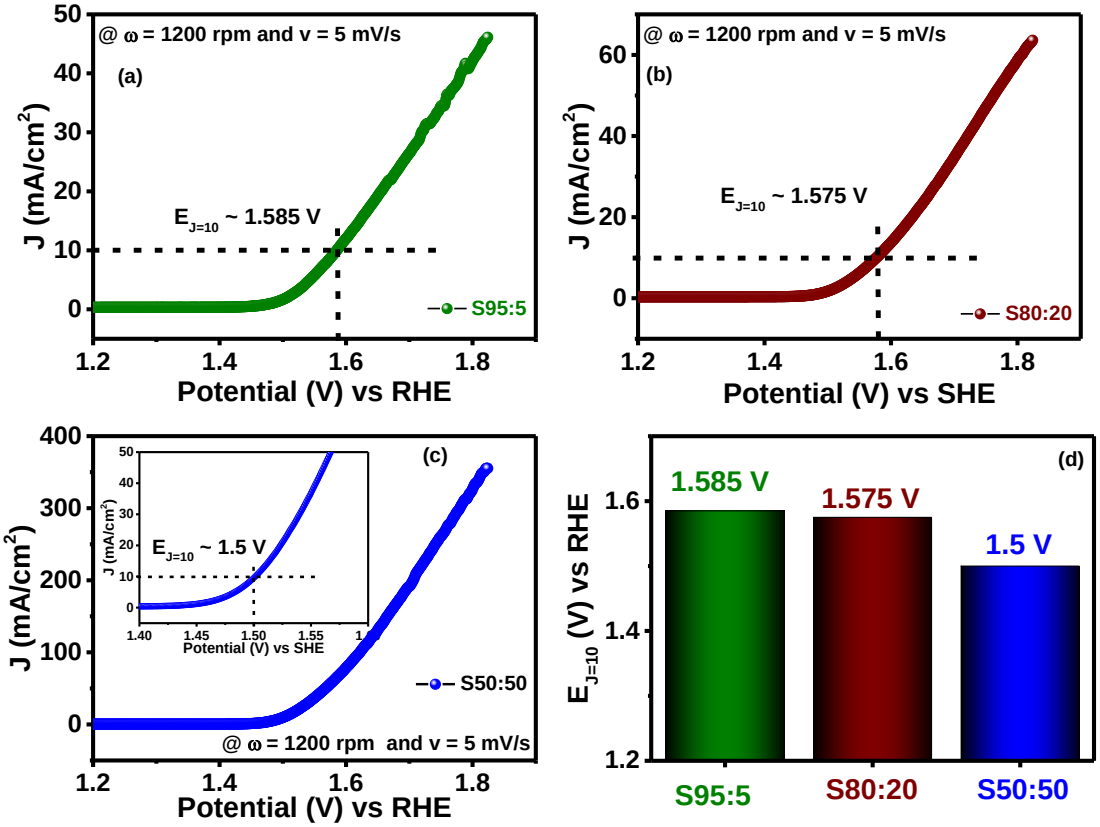

Figure S8. OER polarization curves for (a) S95:5, (b) S80:20 and (c) S50:50, in 30 wt.% KOH aqueous solution. (d) The potential required for different electrocatalysts to achieve a current density of 10 mA/cm^2 as deduced from Figure S8a-c. The experimental findings suggest that S50:50 have comparatively much better electrochemical water oxidation capability under identical experimental conditions.

Table S4. OER activity comparison of graphene-FeCoNiCuCr HEA nanocomposite with various recently reported state-of-the-art metal chalcogenides electrocatalysts in alkaline medium (1 M NaOH/KOH).

Electrocatalysts	**Over potential at J_{OER} = 10 mA/cm^2 (mV)**	**Journals**
CoS_2 nanoparticles	430	Adv. Funct. Mater., 2017, 27, 1701008.
Co_9S_8@MoS_2/CNF	430	Adv. Mater., 2015, 27, 4752–4759.
CoS	361	Electrochem. Commun., 2015, 60, 92–96
MoS_2/Ni_3S_2	420	*Angew. Chem., Int. Ed.* **2016**, *55*, 6702
NiSe nanowires	400	*Angew. Chem., Int. Ed.* **2015**, *54*, 9351.
Mn_3O_3/$CoSe_2$	450	J. Am. Chem. Soc. 2012, 134 (6), 2930-2933.
Ni_33S_2@NC	390	Dalton Trans., 2016, 45, 6352–6356
Co_9S_8/N,S–C	350	Nanoscale, 2017, 9, 12432–12440
Co_9S_8@NOSC	340	Adv. Funct. Mater., 2017, 27, 1606585
Graphene-FeCoNiCuCr HEA nanocomposite	**330**	**Present study**

Table S5. OER activity comparison on graphene-FeCoNiCuCr HEA nanocomposite with various recently reported state-of-the-art metal phosphides electrocatalysts in alkaline medium (1 M NaOH/KOH).

Electrocatalysts	**Over potential at J_{OER} = 10 mA/cm^2 (mV)**	**Journals**
CoP/rGO-400	340 mV	Chem. Rev., 2013, 113, 5782–5816.
NiCoP/C nanoboxes	330 mV	Angew. Chem., Int. Ed., 2017, 56, 3897–3900
Co_2P	370	J. Am. Chem. Soc., 2016, 138, 4006–4009.
CoMnP	330	
CoP/rGO-400	340	Chem. Sci., 2016, 7, 1690–1695.
Co-P/ NC	354	Chem. Mater. 2015, 27 (22), 7636-7642.
Co-P films	345	Angew. Chem. Int. Ed. 2015, 54 (21), 6251-6254.
Graphene-FeCoNiCuCr HEA nanocomposite	**330**	**Present study**

Table S6. OER activity comparison on graphene-FeCoNiCuCr HEA nanocomposite with various recently reported state-of-the-art metal nitrides and borides electrocatalysts in alkaline medium (1 M NaOH/KOH).

Electrocatalysts	**Over potential at J_{OER} = 10 mA/cm^2 (mV)**	**Journals**
Ni_3N nanosheets	350	J. Am. Chem. Soc., 2015, 137, 4119–4125
Co_2N	430	Inorg. Chem. Front., 2016, 3, 236–242.
Co_3N	410	
Co_4N	330	
Ni_3N	430	ChemSusChem, 2010, 3, 169–180.
Amorphous cobalt boride (Co_2B)	367	Angew. Chem., Int. Ed., 2017, 56, 3897–3900.
Amorphous cobalt phyllosilicate	380	Adv. Energy Mater., 2016, 6, 1601189.
Graphene-FeCoNiCuCr HEA nanocomposite	**330**	**Present study**

Table S7. OER activity comparison on graphene-FeCoNiCuCr HEA nanocomposite with various recently reported state-of-the-art oxide based electrocatalysts in alkaline medium (1 M NaOH/KOH).

Electrocatalysts	**Over potential at J_{OER} = 10 mA/cm^2 (mV)**	**Journals**
$CoCr_2O_4$	422	Small, 2016, 12, 2866–2871.
$CoCr_2O_4$/CNT	326	
Co_3O_4	400	RSC Adv., 2016, 6, 2019–2023
$Co_3V_2O_8$	359	J. Mater. Chem. A, 2014, 2, 18435–18443
Co_3O_4	384	
V_2O_5	451	
$CuFe_2O_4$	367	Journal of colloidal and interface science 2019, 540, 59-65
$CoFe_2O_4$	414	
$NiFe_2$ O_4	433	
$NiCo_2O_4$ nanowall arrays	340	*Adv. Energy Mater.* **2017**, *7*, 1602391.
CoOx@CN	385	J. Am. Chem. Soc. 2015, 137 (7), 2688-2694.
Co_3O_4 /$NiCo_2O_4$	340	J. Am. Chem. Soc. 2015, 137 (16), 5590-5595.
N-G-CoO	340	Energy Environ. Sci. 2014, 7 (2), 609-616.
$NixCo_{3-x}$ O_4	370	Adv. Mater. 2010, 22 (17), 1926-1929
$MnCo_2O_x$	410	J. Am. Chem. Soc. 2014, 136 (47), 16481-16484.
MnO_x film	563	J. Am. Chem. Soc. 2012, 134 (41), 17253-17261.
Graphene-FeCoNiCuCr HEA nanocomposite	**330**	**Present study**

Table S8. OER activity comparison on graphene-FeCoNiCuCr HEA nanocomposite with various recently reported state-of-the-art double layered hydroxides (LDH) based electrocatalysts in alkaline medium (1 M NaOH/KOH).

Electrocatalysts	**Over potential at J_{OER} = 10 mA/cm^2 (mV)**	**Journals**
NiCo-LDH	335	Nat. Commun., 2014, 5, 4477.
CoCo-LDH	350	Nat. Commun., 2014, 5, 4477.
NiCo LDH MS	409	Carbon, 2016, 110, 1–7.
Exfoliated NiCo LDH	367	Nano Lett., 2015, 15, 1421–1427
Exfoliated NiCo NS	334	Nat. Commun., 2014, 5, 4477.
CoNiMn LDH/polypyrrole/RGO	369	Nano Res., 2016, 9, 713–725
$Ni_{0.75}Fe_{0.25}$ LDH	350	Nat. Commun., 2016, 7, 11981
Ni_5Mn LDH/MWCNT	350	ACS Appl. Mater. Interfaces, 2016, 8, 14527–14534
Exfoliated CoCo NS	353	Nat. Commun., 2014, 5, 4477
NiCo LDH nanoplates	367	*Nano Lett.* **2015**, *15*, 1421
d-FeOOH nanosheets	390	*Adv. Mater.* **2018**, *30*, 1803144
CoCo LDH	393	Nat. Commun. 2014, 5, 4477
Graphene-FeCoNiCuCr HEA nanocomposite	**330**	**Present study**

Table S9. OER activity comparison on graphene-FeCoNiCuCr HEA nanocomposite with various recently reported state-of-the-art some transition (mono-/multi-) metal based based electrocatalysts in alkaline medium (1 M NaOH/KOH).

Electrocatalysts	**Over potential at J_{OER} = 10 mA/cm^2 (mV)**	**Journals**
CoCx@NC	450	Journal of Catalysis 2019, 371, 185-195
FeCo@NC	480	
N-doped CoCx/FeCo@C/rGO	390	
CoCr(9:1)@NGT	330	*ACS Appl. Energy Mater.*, **2018**, *1* (3), pp 1116–1126
CoCr(7:3)@NGT	362	
Co@NGT	520	
Fe_3C-FeNx enriched carbon sphere	343	*J. Mater. Chem. A, 2018, 6, 8537*
Fe_3C-NCNTs co-embedded boron doped carbon	355	*J. Mater. Chem. A, 2017, **5**, 16843-16853*
Graphene-FeCoNiCuCr HEA nanocomposite	**330**	**Present study**

References

1 R. Nandan, A. Gautam and K. K. Nanda, *J. Mater. Chem. A*, 2018, **6**, 20411–20420.

2 H. R. Devi, R. Nandan and K. K. Nanda, *ACS Appl. Mater. Interfaces*, 2020, **12**, 13888–13895.

3 M. Alanyalioğlu, J. J. Segura, J. Oró-Sol and N. Casañ-Pastor, in *Carbon*, Elsevier Ltd, 2012, vol. 50, pp. 142–152; M. Y. Rekha, N. Mallik and C. Srivastava, Sci. Rep., 2018, **8**, 1.